Multitarget Tracking Algorithms Using Angle Innovations and Extended Kalman Filter

SHENG-YUN HOU[1], HSIEN-SEN HUNG[2], YUAN-CHANG CHANG[3], SHUN-HSYUNG CHANG[4]
[1] Department of Electrical Engineering, National Taiwan Ocean University, and
Department of Electronic Engineering, Hwa Hsia Institute of Technology
111 Gong Jhuan Road, Chung Ho, Taipei County, 23568
Taiwan , R.O.C.
d91530001@mail.ntou.edu.tw
[2]Department of Electrical Engineering, National Taiwan Ocean University
2 Pei-Ning Road, Keelung, Taipei County, 20224
Taiwan , R.O.C.
b0221@mail.ntou.edu.tw
[3]Department of Electronic Engineering, Hwa Hsia Institute of Technology
111 Gong Jhuan Road, Chung Ho, Taipei County, 23568
Taiwan , R.O.C.
ycchang@orion.ee.ntust.edu.tw
[4]Department of Microelectronic Engineering, National Kaohsiung Marine University
142 Haijhuan Road., Nanzih District, Kaohsiung City, 81157
Taiwan , R.O.C.
shchang@mail.ntou.edu.tw

Abstract: - In this paper, we propose a novel angle tracking algorithm, called as FPAT, for tracking multiple narrowband targets. The proposed algorithm modifies the algorithm presented by Park, *et al*. in two ways by using the sensor array output vector rather than the sample covariance matrix and by incorporating the extended Kalman filter instead of a simple Kalman filter. It also applies the prediction characteristic of Kalman filter to prevent the data association problem. The proposed algorithm requires lower computational complexity and also improves the tracking performance especially at lower number of snapshots. Combined with the coherent signal-subspace (CSS) method, the FPAT algorithm is extended to track the direction-of-arrival angles of wideband sources. We also extend the FPAT algorithm to track the range, azimuth, and elevation of each narrowband source in 3-D space. Through computer simulations, the effectiveness of each proposed algorithm is verified.

Key-Words: - Array signal processing, Angle tracking, Extended Kalman Filter (EKF), Direction of arrival.

1 Introduction

Multiple targets tracking is often investigated in sonar, radar, earthquake exploration, air traffic control, remote sensing as well as wireless communications. Target angle-tracking methods, such as the maximum likelihood method [1], the adaptive algorithms [2] and the conjugate gradient search algorithm [3], are computationally very extensive. Sword [4] proposed a recursive angle-tracking method which is computationally simple and can avoid the data association problem. The algorithm, however, has the following disadvantages: (i) Due to recursive approximation used in the substitution process, it will produce the error propagation problem; (ii) Its general use for multiple sources with crossing angles is prohibited because of poor performance. Wang and Wee [5] proposed a simple source tracking scheme by exploiting the fact that the spatial samples on the same wave front have equal amplitude and thus minimum variance. Nikos *et al.* [6, 7] proposed a multistatic target tracking method based on the technique of singular-value decomposition. Marta *et al.* [8] suggested the use of particle filter to track a variable number of objects.

Due to the nature of prediction-correction filtering process, Kalman filter (KF) can reduce estimation error when applied to angle estimation and tracking, as stated in several references, e.g., [9]-[13]. In [9], Rao, *et al.* proposed to estimate angles of targets based on maximum likelihood method as the measurements in KF, which computationally intensive. Besides, the assumption that the signal powers of the targets are all different makes the

algorithm impractical. Javier and Sylvie [10] suggested to estimate angles using the projection approximation subspace tracking algorithm with deflation (PASTd) [14] and a Newton-type method as the measurements in KF. It has lower computational load and better tracking performance than the Rao's algorithm. Park, *et al.* [11] modifies Sword's algorithm by using predicated angle estimates, instead of existing angle estimates, for calculation of angle innovations. In order to avoid abnormally large angle innovations when the target angles are very close, a modified least-squares solution is used. The resultant angle innovations are then used in KF to update the angle estimates for improving the tracking performance. However, tracking performance degrades seriously with an increasing number of crossing targets. As such, Ryu, *et al.* [12, 13] suggested to obtain the angle innovations of the targets from a signal subspace, instead of the sensor output covariance matrix, via PASTd algorithm [14]. In [15], the neural extended Kalman filter, which is an adaptive state estimation routine, was proposed to aid in the tracking through maneuvers in target-tracking systems.

All the above algorithms are based on the sample covariance matrix or signal subspace made with a block of measurement snapshots from a sensor array. Some of them require the estimation of target angles as the measurement angles in the Kalman filter at each time step, resulting in large computational load especially when the number of snapshots increases. In order to relieve huge computational burden, the sensor array output is directly used as the measurement data in the extended Kalman filter (EKF), rather than the angle estimates are indirectly used as the measurement data in the Kalman filter. Kong and Chun [16] proposed a fast angle-tracking algorithm based on a single number of snapshot and EKF. However, the algorithm has low tracking success rate when targets approaches near the points of intersection. To overcome the drawbacks mentioned above, we firstly propose a fast predictive angle-tracking algorithm, named the FPAT algorithm, for tracking multiple narrowband sources in 2-D space. As demonstrated by computer simulations, it has lower computational complexity and better tracking performance than the Park's [11] and Kong's [16] algorithms. The FPAT algorithm is then extended to track narrowband sources in 3-D space.

All the aforementioned methods are applicable to track narrowband signals but fail to track wideband signals. In many practical situations such as sonar, signals are wideband. For tracking wideband sources, we propose a method which combines the FPAT algorithm with the coherent signal subspace method (CSS) [17]. In the following context, section 2 first describes the FPAT algorithm for tracking multiple narrowband sources in 2-D space and then extended to narrowband sources in 3-D space. Section 3 proposes a tracking algorithm for wideband sources. Section 4 demonstrates the tracking performances via computer simulations. Section 5 draws the conclusion.

2 The Proposed Narrowband Tracking Algorithm

2.1 Data model for narrowband sources in 2-D space

Consider that there are N moving targets from which narrowband signals of a common angular frequency ω are radiated, propagated and received by $M(>N)$ sensors. The sensors are deployed as a uniform linear array with interelement spacing d. The output of the m-th sensor for the k-th sampling interval is

$$r_m(k) = \sum_{i=1}^{N} e^{-j\omega\tau_{mi}(k)} s_i(k) + n_m(k)$$

where $s_i(k)$ is the signal transmitted by the i-th source; $\tau_{mi}(k)$ is the difference in time delays of the i-th source to reach the first (reference) and the m-th sensors. $n_m(k)$ is the white Gaussian noise with zero mean and variance σ^2, uncorrelated with the source signals. Assume all sources are coplanar with the sensor array and are in the far field. The time delay, expressed as a function of direction angle, is given by $\tau_{mi}(k)=(\frac{d}{c})(m\text{-}1)\sin(\theta_i(k))$, where $\theta_i(k)$ is the direction angle of the i-th source and c is the wave speed. By using vector-matrix representation, the output of the sensor array is

$$\mathbf{r}(k) = \mathbf{A}(k)\mathbf{s}(k) + \mathbf{n}(k) \qquad (1)$$

where $\mathbf{r}(k) = [r_1(k), r_2(k), ..., r_M(k)]^T$ is the output vector, $\mathbf{s}(k) = [s_1(k), s_2(k), ..., s_N(k)]^T$ is the signal vector, $\mathbf{n}(k) = [n_1(k), n_2(k), ..., n_M(k)]^T$ is the noise vector. The superscript T is the transpose operator. The $M\times N$ direction matrix $\mathbf{A}(k)$ is defined as

$$\mathbf{A}(k)=\begin{bmatrix} 1 & 1 & \cdots & 1 \\ \gamma_1(k) & \gamma_2(k) & \cdots & \gamma_N(k) \\ \vdots & \vdots & \ddots & \vdots \\ \gamma_1^{M-1}(k) & \gamma_2^{M-1}(k) & \cdots & \gamma_N^{M-1}(k) \end{bmatrix} \qquad (2)$$

where

$$\gamma_i(k) = e^{-j\omega(\frac{d}{c})\sin\theta_i(k)} \text{ for } i = 1, 2, \ldots, N.$$

Based on the data model of (1), we are to track the direction-of-arrival angles (DOAs) $\theta_i(k)$, i =1, 2, …, N. Suppose there are L measurements (snapshots) that are taken for each increment T_s, and the time increment is sufficiently small allowing us to approximate the target as stationary within each time increment. The tracking problem is aimed at estimating $\theta_i(t)$, t=Ts, $2Ts$,… (equivalently, $\theta_i(k)$, k=1, 2,…), i =1, 2, …, N. from L snapshots of array data measured within each time increment T_s .

2.2 The Fast Predictive Angle Tracking (FPAT) algorithm

For tracking nonstationary targets efficiently and effectively, the Fast Predictive Angle Tracking (FPAT) algorithm is presented. In the proposed algorithm, the sensor array output is used as measurement data in EKF, instead of KF, since the measurement model is nonlinear in terms of angle estimates. Using the predicted angles, the FPAT algorithm modifies the Park's method to obtain angular innovation, from which the angle estimates are updated (smoothed) via Kalman gain. The FPAT algorithm is stated as follows. First, we describe the discrete-time state (process) model for the target motion described in the previous section. For each time index k, we define the state vector for the i-th target as $\mathbf{x}_i(k) = \begin{bmatrix} \theta_i(k) & \dot{\theta}_i(k) \end{bmatrix}^T$, consisting of its DOA and angular speed. The target motion can lead to the process equation [11]

$$\mathbf{x}_i(k+1) = \mathbf{F}\mathbf{x}_i(k) + \mathbf{w}_i(k) \quad (3)$$

$$\mathbf{F} = \begin{bmatrix} 1 & T_s \\ 0 & 1 \end{bmatrix}$$

where $\mathbf{w}_i(k)$ is the process noise vector and is assumed to be Gaussian distributed with zero mean and covariance

$$\mathbf{Q}_i = \sigma_w^2 \begin{bmatrix} \frac{T_s^3}{3} & \frac{T_s^2}{2} \\ \frac{T_s^2}{2} & T_s \end{bmatrix}$$

Assume that the motion of each target is mutually independent. By defining the composite state vector as $\mathbf{x}(k) = \begin{bmatrix} \mathbf{x}_1^T(k),...,\mathbf{x}_N^T(k) \end{bmatrix}^T$, the system dynamics is governed by the process model

$$\mathbf{x}(k+1) = \bar{\mathbf{F}}\mathbf{x}(k) + \mathbf{w}(k) \quad (4)$$

$$\bar{\mathbf{F}} = diag(\overbrace{\mathbf{F},\cdots,\mathbf{F}}^{N})$$

The process noise vector $\mathbf{w}(k)$ reflects the random modeling error, which is Gaussian distributed with zero mean vector and covariance

$$\bar{\mathbf{Q}} = diag(\mathbf{Q}_1,\cdots,\mathbf{Q}_N)$$

The matrices $\bar{\mathbf{F}}$ and $\bar{\mathbf{Q}}$ are all block diagonal. Although the process equation is a linear model, the measurement model of (1) is a vector nonlinear function of the target DOAs (and thus, of the target state vectors as well), which can be restated as

$$\mathbf{r}(k) \triangleq \mathbf{h}(\mathbf{x}(k),\mathbf{s}(k),\mathbf{n}(k)) = \mathbf{A}(\mathbf{x}(k))\mathbf{s}(k) + \mathbf{n}(k) \quad (5)$$

,where $\mathbf{n}(k)$ is complex Gaussian noise process with the known covariance $\sigma_n^2\mathbf{I}$, and is assumed to be uncorrelated with the process noise $\mathbf{w}(k)$. Under the assumption of a uniform linear array with a half wavelength of interelement spacing, the partial derivative matrix of the measurement model (5) is given by

$$\mathbf{H}(k) = \frac{\partial \mathbf{h}}{\partial \mathbf{x}}\Big|_{\mathbf{x}=\mathbf{x}(k|k-1)} = [\mathbf{H}_1(k),...,\mathbf{H}_N(k)]\Big|_{\mathbf{x}=\mathbf{x}(k|k-1)}$$

By augmenting the real and imaginary parts of each complex matrix $\mathbf{H}_i(k)$, we have the composite real matrix of dimension $2M\times 2N$

$$\bar{\mathbf{H}}(k) = \begin{bmatrix} real(\mathbf{H}_1(k),...,\mathbf{H}_N(k)) \\ imag(\mathbf{H}_1(k),...,\mathbf{H}_N(k)) \end{bmatrix}_{\mathbf{x}=\mathbf{x}(k|k-1)}$$

which can be expressed as

$$\bar{\mathbf{H}}(k) = \begin{bmatrix} 0 & 0 & \cdots & 0 & 0 \\ g_{1,1} & 0 & \cdots & g_{N,1} & 0 \\ \vdots & \vdots & \ddots & \vdots & \vdots \\ g_{1,M-1} & 0 & \cdots & g_{N,M-1} & 0 \\ 0 & 0 & \cdots & 0 & 0 \\ c_{1,1} & 0 & \cdots & c_{N,1} & 0 \\ \vdots & \vdots & \ddots & \vdots & \vdots \\ c_{1,M-1} & 0 & \cdots & c_{N,M-1} & 0 \end{bmatrix}_{\mathbf{x}=\mathbf{x}(k|k-1)}$$

where

$$g_{i,b} = -\sin(\pi b \sin(\theta_i(k)))\cos(\theta_i(k))s_i(k) \quad (6)$$

$$c_{i,b} = -\cos(\pi b \sin(\theta_i(k)))\cos(\theta_i(k))s_i(k) \quad (7)$$

i=1, …, N, b=1, …, M-1.

Initially (at k=0), the target DOAs, $\{\hat{\theta}_i(-1)\}$ and $\{\hat{\theta}_i(0)\}$ at two successive time instants, k=-1 and k=0, are assumed to be available, which can be estimated by any kind of angle estimation algorithm (for instance the MUSIC algorithm [18]). Thus, the initial state vector estimate can be set as $\hat{\mathbf{x}}(0|0) = [\hat{\theta}_1(0) \quad (\hat{\theta}_1(0) - \hat{\theta}_1(-1))/T_s, \cdots, \quad \hat{\theta}_N(0)$

$(\hat{\theta}_N(0) - \hat{\theta}_N(-1))/T_s]^T$ with its covariance matrix $\mathbf{P}(0|0)$, given by

$$\mathbf{P}(0\,|\,0) = \sigma_v^2 \begin{bmatrix} 1 & \frac{1}{T_s} & & & 0 \\ \frac{1}{T_s} & \frac{2}{T_s^2} & & & \\ & \ddots & \ddots & & \\ & & & 1 & \frac{1}{T_s} \\ 0 & & & \frac{1}{T_s} & \frac{2}{T_s^2} \end{bmatrix}$$

The proposed tracking algorithm can be summarized in the following four steps.

Step I. Prediction of angles

The prediction of the state vector and its covariance matrix can be obtained from the existing estimates by the equations

$$\hat{\mathbf{x}}(k\,|\,k-1) = \overline{\mathbf{F}}\hat{\mathbf{x}}(k-1\,|\,k-1) \quad (8)$$

$$\mathbf{P}(k\,|\,k-1) = \overline{\mathbf{F}}\mathbf{P}(k-1\,|\,k-1)\overline{\mathbf{F}}^T + \overline{\mathbf{Q}} \quad (9)$$

The first element of each state vector $\hat{\mathbf{x}}_i(k\,|\,k-1)$ is the predicted estimate $\hat{\theta}_i(k\,|\,k-1)$ of $\theta_i(k)$. The predicted direction matrix $\mathbf{A}(k|k\text{-}1)$ can be obtained by (2) using $\hat{\theta}_i(k\,|\,k-1)$ for $\theta_i(k)$. From (1), the predicted output of the sensor array becomes

$$\mathbf{r}(k\,|\,k-1) = \mathbf{A}(k\,|\,k-1)\mathbf{s}(k) \quad (10)$$

Using maximum likelihood method, $\mathbf{s}(k)=[s_1(k),\ldots, s_N(k)]^T$ in (10) can be estimated by

$$\hat{\mathbf{s}}(k) = \left[\mathbf{A}^H(\hat{\theta}(k\,|\,k-1))\ \mathbf{A}(\hat{\theta}(k\,|\,k-1))\right]^{-1}\mathbf{A}^H(\hat{\theta}(k\,|\,k-1))\mathbf{r}(k) \quad (11)$$

Step II. Computations of the angle innovation

After time T_s, the direction matrix is obtained from a new array output as

$$\mathbf{A}(k) = \mathbf{A}(k\,|\,k-1) + \delta\mathbf{A}(k) \quad (12)$$

where $\delta\mathbf{A}(k)$ is the error matrix which can be derived, according to Sword [4], as

$$\delta\mathbf{A}(k) = \begin{bmatrix} 0 & \cdots & 0 \\ \delta\gamma_1 & \cdots & \delta\gamma_N \\ 2\gamma_1\delta\gamma_1 & \cdots & 2\gamma_N\delta\gamma_N \\ \vdots & \ddots & \vdots \\ (M-1)\gamma_1^{M-2}\delta\gamma_1 & \cdots & (M-1)\gamma_N^{M-2}\delta\gamma_N \end{bmatrix} \quad (13)$$

wherein

$$\delta\gamma_i(k) = -j\pi\cos\theta_i(k)\gamma_i(k)\delta\theta_i(k) \quad (14)$$

Based on (1), the residual array output $\Delta\mathbf{r}(k)$ can be obtained from (10) as

$$\Delta\mathbf{r}(k) = \mathbf{r}(k) - \mathbf{r}(k\,|\,k-1) = \delta\mathbf{A}(k)\mathbf{s}(k) + \mathbf{n}(k) \quad (15)$$

Notice that the first row vector of $\delta\mathbf{A}(k)$ in (13) is a null vector. In order to reduce the computation, the null vector allows us to define a $(M\text{-}1)\times 1$ vector $\Delta\tilde{\mathbf{r}}$, which is obtained by removing the first element of $\Delta\mathbf{r}$ in (15). By substituting (14) into (13), $\Delta\tilde{\mathbf{r}}$ can be represented by (dropping k temporarily)

$$\Delta\tilde{\mathbf{r}} = \mathbf{B}\delta\theta + \tilde{\mathbf{n}} \quad (16)$$

where the $(M\text{-}1)\times N$ matrix $\mathbf{B}$ is

$$\mathbf{B} = -j\pi\begin{bmatrix} \cos(\theta_1)\gamma_1 s_1 & \cdots & \cos(\theta_N)\gamma_N s_N \\ 2\cos(\theta_1)\gamma_1^2 s_1 & \cdots & 2\cos(\theta_N)\gamma_N^2 s_N \\ \vdots & \ddots & \vdots \\ (M-1)\cos(\theta_1)\gamma_1^{M-1}s_1 & \cdots & (M-1)\cos(\theta_N)\gamma_N^{M-1}s_N \end{bmatrix}$$

wherein θ_i is substituted with the predicted angle $\hat{\theta}_i(k\,|\,k-1)$, and $\delta\theta = [\delta\theta_1(k), \delta\theta_2(k),\cdots, \delta\theta_N(k)]$ is the unknown angle innovation vector to be estimated. In general, a least-squares solution, $\delta\theta = (\mathbf{B}^H\mathbf{B})^{-1}\mathbf{B}^H\Delta\tilde{\mathbf{r}}$, can be obtained using (16). However, a modified solution

$$\delta\theta = (\mathbf{B}^H\mathbf{B} + \mathbf{L})^{-1}\mathbf{B}^H\Delta\tilde{\mathbf{r}} \quad (17)$$

as suggested in Park's algorithm, will be used to constrain the absolute values of innovations for the cases of nearby targets, where $\mathbf{L}$ is a weighting matrix with diagonal form. It should be noticed that s_i, i=1,$\cdots$, N, in $\mathbf{B}$ are obtained from (11).

Step III. Estimation of the angles

The estimated angle can be obtained as

$$\hat{\theta}_i(k) = \hat{\theta}_i(k\,|\,k-1) + \delta\theta_i(k) \quad (18)$$

Furthermore, $\hat{\theta}_i(k)$ and $\hat{s}_i(k)$ are substituted into (6) and (7) to update the matrix $\overline{\mathbf{H}}(\mathrm{k})$.

Step IV. Smoothing the estimated angles

Since the state vector is real-valued, we formulate the state estimation equation as

$$\hat{\mathbf{x}}(k\,|\,k) = \hat{\mathbf{x}}(k\,|\,k-1) + \mathbf{K}\Delta\overline{\mathbf{r}}(k) \quad (19)$$

where $\Delta\bar{\mathbf{r}}(k)=[\Delta\mathbf{r}_R\ \Delta\mathbf{r}_I]^T$ is a real vector; $\Delta\mathbf{r}_R$ and $\Delta\mathbf{r}_I$ are the real and imaginary parts of $\Delta\mathbf{r}(k)$ from (15). $\mathbf{K}$ is the Kalman Gain matrix, given by

$$\mathbf{K}=\mathbf{P}(k\,|\,k-1)\bar{\mathbf{H}}^T\left[\bar{\mathbf{H}}\mathbf{P}(k\,|\,k-1)\bar{\mathbf{H}}^T+\sigma_n^2\mathbf{I}\right]^{-1} \quad (20)$$

The covariance matrix of $\hat{\mathbf{x}}(k\,|\,k)$ is given by

$$\mathbf{P}(k\,|\,k)=\left[\mathbf{I}-\mathbf{K}\bar{\mathbf{H}}\right]\mathbf{P}(k\,|\,k-1) \quad (21)$$

The proposed FPAT algorithm requires the number of $7MN^2+16M^2N+MNL$ real multiplications, whereas the Park's algorithm [11] and the Kong's algorithm [16] require the numbers of $3MN^2+L(3M^2+MN)$ and $5N^3+10MN^2+8M^2N+MNL$ real multiplications respectively (L is the number of snapshots). Table 1 shows the comparison of computational complexity among these algorithms for N=3, M=8 and different number of snapshots. It is evident that the FPAT algorithm has lower computational complexity than Park's algorithm for $L \geq 30$, where $L \geq 30$ is often needed for acceptable tracking performance. Although the computational complexity is higher than the Kong's algorithm, the proposed method has much better performance as demonstrated by the simulations.

Table 1. Computational complexity comparison for N=3, M=8 and different L values.

Algorithm		FPAT	Park's	Kong's
Number of real multiplications	L=1	3600	432	2415
	L=10	3816	2376	2631
	L=30	4296	6696	3111
	L=50	4776	11016	3591

2.3 The FPAT algorithm for tracking targets in 3-D space

The FPAT algorithm is now extended to track narrowband targets in 3-D space, where the coordinate system is shown in Fig. 1. $s_i(k)$ is the signal transmitted by the i-th target of which φ_i and θ_i are the azimuth and elevation respectively. ρ_i is the range from the i-th target to the first (reference) sensor in the uniform linear array. To be explained later, the number of sensors M must satisfy the condition $M \geq 3N+1$, where N is the number of targets. All the targets can be located in the near field or far field. In the following formulations, far-field targets are treated.

The output of the m-th sensor for the k-th sampling interval can be expressed as

$$r_m(k)=\sum_{i=1}^{N}s_i(k-\tau_{mi}(k))+n_m(k) \qquad m=1,2,\cdots,M \quad (22)$$

From the array and source configurations shown in Fig. 1, $\tau_{mi}(k)$ can be expressed as

$$\tau_{mi}(k)=\frac{1}{c}\left[\sqrt{(p_i-x_m)^2+(q_i-y_m)^2+(l_i-z_m)^2}-\rho_i\right]$$

where (x_m, y_m, z_m) is the m-th sensor position relative to the reference sensor. Here $x_m=(m-1)d$, $y_m=0$, and $z_m=0$. The location coordinate of the i-th signal source is given by

$$p_i=\rho_i\sin\theta_i\cos\varphi_i$$
$$q_i=\rho_i\sin\theta_i\sin\varphi_i$$
$$l_i=\rho_i\cos\theta_i$$

Assume that all the signal sources are narrowband with a common angular frequency ω. Then

$$s(k-\tau_{mi}(k))\simeq s(k)e^{-j\omega\tau_{mi}(k)}$$

Therefore, (22) becomes

$$r_m(k)=\sum_{i=1}^{N}e^{-j\omega\tau_{mi}(k)}s_i(k)+n_m(k) \qquad m=1,2,\cdots,M$$

In vector-matrix notation, the received output vector of the sensor array is $\mathbf{r}(k)=\mathbf{A}(k)\mathbf{s}(k)+\mathbf{n}(k)$, where

$$\mathbf{A}(k)=\begin{bmatrix}1 & 1 & \cdots & 1\\ \gamma_{21}(k) & \gamma_{22}(k) & \cdots & \gamma_{2N}(k)\\ \vdots & \vdots & \ddots & \vdots\\ \gamma_{M1}(k) & \gamma_{M2}(k) & \cdots & \gamma_{MN}(k)\end{bmatrix}$$

and

$$\gamma_{mi}(k)=e^{-j\omega\tau_{mi}(k)}$$

Let $\delta\rho(k)$, $\delta\varphi(k)$, and $\delta\theta(k)$ be the unknown variations of $\rho(k)$, $\varphi(k)$, $\theta(k)$ respectively, from time k-1 to time k. These variations will produce the variations $\Delta\mathbf{r}(k)$ and $\delta\mathbf{A}(k)$, where $\Delta\mathbf{r}(k)=\mathbf{r}(k)-\mathbf{r}(k|k\text{-}1)$, and $\delta\mathbf{A}(k)=\mathbf{A}(k)-\mathbf{A}(k|k\text{-}1)$. Basically, the equations (8)-(12), (15) and (19)-(21) remain unchanged except (13)-(14) and (16)-(18) are changed as follows.

The (m,n) element of $\delta\mathbf{A}(k)$ can be derived as

$$[\delta\mathbf{A}(k)]_{(m,n)}=-j\omega\gamma_{mn}(k)\left[\frac{\partial\tau_{mn}}{\partial\rho_n}\delta\rho_n+\frac{\partial\tau_{mn}}{\partial\varphi_n}\delta\varphi_n+\frac{\partial\tau_{mn}}{\partial\theta_n}\delta\theta_n\right]$$

where

$$\frac{\partial\tau_{mn}}{\partial\rho_n}=\frac{1}{c}\left\{\left[\rho_n\sin\theta_n\cos\varphi_n-(m-1)d\right]^2+\left(\rho_n\sin\theta_n\sin\varphi_n\right)^2+\left(\rho_n\cos\theta_n\right)^2\right\}^{-\frac{1}{2}}$$
$$\times\left[\rho_n-(m-1)d\sin\theta_n\cos\varphi_n\right]-\frac{1}{c}$$

$$\frac{\partial\tau_{mn}}{\partial\varphi_n}=\frac{1}{c}\left\{\left[\rho_n\sin\theta_n\cos\varphi_n-(m-1)d\right]^2+\left(\rho_n\sin\theta_n\sin\varphi_n\right)^2+\left(\rho_n\cos\theta_n\right)^2\right\}^{-\frac{1}{2}}$$
$$\times(m-1)d\rho_n\sin\theta_n\sin\varphi_n$$

$$\frac{\partial\tau_{mn}}{\partial\theta_n}=\frac{1}{c}\left\{\left[\rho_n\sin\theta_n\cos\varphi_n-(m-1)d\right]^2+\left(\rho_n\sin\theta_n\sin\varphi_n\right)^2+\left(\rho_n\cos\theta_n\right)^2\right\}^{-\frac{1}{2}}$$
$$\times-(m-1)d\rho_n\cos\theta_n\cos\varphi_n$$

and

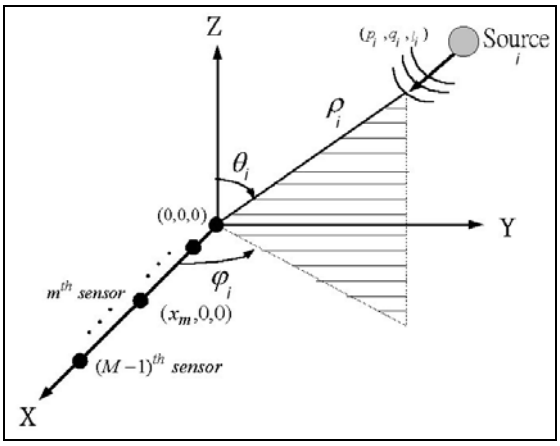

Fig. 1 Sensor array and source configurations in 3-D space.

$$\Delta\tilde{\mathbf{r}}(k)=\mathbf{B}\cdot\begin{bmatrix}\delta\rho(k)\\ \delta\varphi(k)\\ \delta\theta(k)\end{bmatrix}+\tilde{\mathbf{n}} \qquad (23)$$

where the matrix **B** is a (M-1) × 3N matrix, given by

$$-j\omega\begin{bmatrix}\gamma_{21}\frac{\partial\tau_{21}}{\partial\rho_1}s_1 & \cdots & \gamma_{2N}\frac{\partial\tau_{2N}}{\partial\rho_1}s_N & \gamma_{21}\frac{\partial\tau_{21}}{\partial\varphi_1}s_1 & \cdots & \gamma_{2N}\frac{\partial\tau_{2N}}{\partial\varphi_1}s_N & \gamma_{2N}\frac{\partial\tau_{21}}{\partial\theta_1}s_1 & \cdots & \gamma_{2N}\frac{\partial\tau_{2N}}{\partial\theta_1}s_N\\ \vdots & \ddots & \vdots & \vdots & \ddots & \vdots & \vdots & \ddots & \vdots\\ \gamma_{M1}\frac{\partial\tau_{M1}}{\partial\rho_1}s_1 & \cdots & \gamma_{M1}\frac{\partial\tau_{MN}}{\partial\rho_1}s_N & \gamma_{M1}\frac{\partial\tau_{M1}}{\partial\varphi_1}s_1 & \cdots & \gamma_{M1}\frac{\partial\tau_{MN}}{\partial\varphi_1}s_N & \gamma_{M1}\frac{\partial\tau_{M1}}{\partial\theta_1}s_1 & \cdots & \gamma_{MN}\frac{\partial\tau_{MN}}{\partial\theta_1}s_N\end{bmatrix}$$

$\delta\rho(k)$=[$\delta\rho_1(k)$, ⋯ , $\delta\rho_N(k)$]^T, $\delta\varphi(k)$=[$\delta\varphi_1(k)$, ⋯ , $\delta\varphi_N(k)$]^T, and $\delta\theta(k)$=[$\delta\theta_1(k)$, ⋯ , $\delta\theta_N(k)$]^T are obtained by

$$\begin{bmatrix}\delta\rho(k)\\ \delta\varphi(k)\\ \delta\theta(k)\end{bmatrix}=(\mathbf{B}^H\mathbf{B}+\mathbf{L})^{-1}\mathbf{B}^H\Delta\tilde{\mathbf{r}}$$

and used to update the state estimation according to

$$\hat{\theta}_i(k)=\hat{\theta}_i(k\,|\,k-1)+\delta\theta_i(k)$$
$$\hat{\varphi}_i(k)=\hat{\varphi}_i(k\,|\,k-1)+\delta\varphi_i(k)$$
$$\hat{\rho}_i(k)=\hat{\rho}_i(k\,|\,k-1)+\delta\rho_i(k)$$

It should be noted that there is one limiting condition, i.e., M-1 ≥ 3N, under which the M-1 linear equations are used for solving 3N unknown variables.

3 The Proposed Wideband Tracking Algorithm

3.1 Data model for wideband sources in 2-D space

For a narrowband source, the phase delay of the received signal is only related to the distance between the receiving sensor and the reference sensor as well as the bearing of the source. However, for a wideband source, the phase delay of the received signal is also related to frequency. Therefore, the data model represented in frequency domain is more appropriate. Considering that signals from N far-field wideband sources with bandwidth Bw are received by a uniform linear array with M (>N) sensors. The signal received by the m-th sensor can be represented as follows

$$r_m(k)=\sum_{i=1}^{N}s_i(k-\tau_{mi}(k))+n_m(k) \qquad (24)$$

and

$$\tau_{mi}(k)=\frac{d(m-1)\sin\theta_i}{f_0\lambda_0}$$

where f_0 is the center frequency of the entire band and λ_0 is the wavelength associated with the center frequency. By taking Fourier transform on both sides of (24), the j-th frequency component of $r_m(k)$ is given by: (assume $d=\frac{1}{2}\lambda_0$)

$$\begin{aligned}r_m(f_j) &= \sum_{i=1}^{N}s_i(f_j)e^{-j2\pi f_j\tau_{mi}}+n_m(f_j) \qquad j=1,\cdots,J\\ &= \sum_{i=1}^{N}s_i(f_j)e^{-j\pi(m-1)(\frac{f_j}{f_0})\sin\theta_i}+n_m(f_j)\end{aligned}$$

The vector representation is shown as

$$\mathbf{r}(f_j)=\mathbf{A}(f_j)\mathbf{s}(f_j)+\mathbf{n}(f_j) \qquad (25)$$

where

$$\mathbf{r}(f_j)=[r_1(f_j),r_2(f_j),...,r_M(f_j)]^T$$
$$\mathbf{s}(f_j)=[s_1(f_j),s_2(f_j),...,s_N(f_j)]^T$$
$$\mathbf{n}(f_j)=[n_1(f_j),n_2(f_j),...,n_M(f_j)]^T$$

The M×N direction matrix $\mathbf{A}(f_j)$ is defined as:

$$\mathbf{A}(f_j)=\begin{bmatrix}1 & 1 & \cdots & 1\\ \gamma_1(f_j) & \gamma_2(f_j) & \cdots & \gamma_N(f_j)\\ \vdots & \vdots & \ddots & \vdots\\ \gamma_1^{M-1}(f_j) & \gamma_2^{M-1}(f_j) & \cdots & \gamma_N^{M-1}(f_j)\end{bmatrix} \qquad (26)$$

where

$$\gamma_i(f_j)=e^{-j\pi(\frac{f_j}{f_0})\sin\theta_i} \quad i=1, 2, \ldots, N.$$

The covariance matrix of $\mathbf{r}(f_j)$ is

$$\mathbf{R}(f_j)=E[\mathbf{r}(f_j)\mathbf{r}^H(f_j)]=\mathbf{A}(f_j)\mathbf{S}(f_j)\mathbf{A}^H(f_j)+\sigma^2(f_j)\mathbf{I} \qquad (27)$$

where $\mathbf{S}(f_j)$ is the covariance matrix of $\mathbf{s}(f_j)$.

3.2 Coherent Signal-Subspace (CSS) method

The main idea of the coherent signal-subspace method [17] is to utilize the focusing matrix which transfers the direction matrix at each sub-band frequency to the one at the center frequency f_0, so that the covariance matrix in (27) is transformed accordingly. By averaging the transformed covariance matrix for each band, the resultant covariance matrix can be used by any high resolution narrowband bearing estimating algorithm to determine the directions of all sources.

The CSS method, in theory, is to use the focusing matrix $\mathbf{T}(f_j)$, satisfying [17]

$$\mathbf{T}(f_j)\mathbf{A}(f_j) = A(f_0)\ j=1, 2, \ldots, J. \tag{28}$$

Hung and Kaveh [19] proposed a unitary focusing matrix based on the following criterion:

$$\begin{aligned} &\min_{\mathbf{T}(f_j)} \left\| \mathbf{A}(f_0) - \mathbf{T}(f_j)\mathbf{A}(f_j) \right\|_F^2 \qquad j = 1,2,\cdots,J \\ &s.t. \quad \mathbf{T}^H(f_j)\mathbf{T}(f_j) = \mathbf{T}(f_j)\mathbf{T}^H(f_j) = \mathbf{I} \end{aligned} \tag{29}$$

The solution for (29) is

$$\mathbf{T}(f_j) = \mathbf{V}(f_j)\mathbf{U}(f_j) \qquad j = 1,2,\cdots,J \tag{30}$$

where $\mathbf{V}(f_j)$ and $\mathbf{U}(f_j)$ are the left singular and right singular vectors of $\mathbf{A}(f_0)\mathbf{A}^H(f_j)$. Finally, the coherently averaged covariance matrix

$$\bar{\mathbf{R}} = \sum_{j=1}^{J} \mathbf{T}(f_j)\mathbf{R}(f_j)\mathbf{T}^H(f_j) \tag{31}$$

is processed by a narrowband bearing estimation algorithm such as MUSIC [18].

3.2 The wideband FPAT tracking algorithm

For the purpose of tracking wideband signals, the traditional bearing estimation algorithms should perform eigendecomposition once a new single or block of data is available. It is very time-consuming. Besides, they fail to analyze the signals which are close to the crossing point. Consequently, in order to overcome the stated problems, a tracking algorithm, which incorporates the CSS method with unitary focusing matrix into the FPAT algorithm, is proposed.

The execution of the proposed wideband FPAT tracking algorithm is divided into four steps.

Step I. Prediction of angles

As described in Section 2, the predicted angle $\hat{\theta}_i(k \mid k-1)$ can be obtained from (8). At time k, the predicted direction matrix $\mathbf{A}(k|k\text{-}1,f_j)$ is given by

$$\mathbf{A}(k \mid k-1, f_j) = \begin{bmatrix} 1 & \cdots & 1 \\ e^{-j\pi(\frac{f_j}{f_0})\sin\hat{\theta}_1(k|k-1)} & \cdots & e^{-j\pi(\frac{f_j}{f_0})\sin\hat{\theta}_N(k|k-1)} \\ \vdots & \ddots & \vdots \\ e^{-j\pi(M-1)(\frac{f_j}{f_0})\sin\hat{\theta}_1(k|k-1)} & \cdots & e^{-j\pi(M-1)(\frac{f_j}{f_0})\sin\hat{\theta}_N(k|k-1)} \end{bmatrix}$$

and the predicted array output is

$$\mathbf{r}(k \mid k-1, f_j) = \mathbf{A}(k \mid k-1, f_j)\mathbf{s}(f_j) \tag{32}$$

Step II. Computations of the angle innovation

The direction matrix at time k is updated as

$$\mathbf{A}(k, f_j) = \mathbf{A}(k \mid k-1, f_j) + \delta\mathbf{A}(f_j) \tag{33}$$

using a new array output of

$$\mathbf{r}(k, f_j) = \mathbf{A}(k, f_j)\mathbf{s}(f_j) + \mathbf{n}(k, f_j) \tag{34}$$

Using the focusing matrix $\mathbf{T}(f_j)$ of (30), (32) and (34) become

$$\begin{aligned} \mathbf{Y}(k \mid k-1, f_0) &= \sum_{j=1}^{J} \mathbf{T}(f_j)\mathbf{A}(k \mid k-1, f_j)\mathbf{s}(f_j) \\ &= \mathbf{A}(k \mid k-1, f_0)\hat{\mathbf{s}} \end{aligned} \tag{35}$$

$$\mathbf{Y}(k, f_0) = \sum_{j=1}^{J} \mathbf{T}(f_j)\mathbf{r}(k, f_j) = \mathbf{A}(k, f_0)\hat{\mathbf{s}} + \bar{\mathbf{n}}(k) \tag{36}$$

where $\hat{\mathbf{s}} = \sum_{j=1}^{J} \mathbf{s}(f_j)$ and $\bar{\mathbf{n}}(k) = \sum_{j=1}^{J} \mathbf{T}(f_j)\mathbf{n}(k, f_j)$.

From (35) and (36), we have

$$\Delta\mathbf{Y}(k) = \mathbf{Y}(k, f_0) - \mathbf{Y}(k \mid k-1, f_0) = \delta\mathbf{A}(k)\hat{\mathbf{s}} + \bar{\mathbf{n}}(k) \tag{37}$$

where

$$\delta\mathbf{A}(k) = \begin{bmatrix} 0 & \cdots & 0 \\ \delta\gamma_1 & \cdots & \delta\gamma_N \\ 2\gamma_1\delta\gamma_1 & \cdots & 2\gamma_N\delta\gamma_N \\ \vdots & \ddots & \vdots \\ (M-1)\gamma_1^{M-2}\delta\gamma_1 & \cdots & (M-1)\gamma_N^{M-2}\delta\gamma_N \end{bmatrix}$$

and $\delta\gamma_i(k) = -j\pi\cos\theta_i(k)\gamma_i(k)\delta\theta_i(k)$. As discussed previously, $\delta\theta$ can be obtained from (17).

Step III. Estimation of the angles

The estimated angle can be obtained according to (18). Furthermore, $\hat{\theta}_i(k)$ is substituted into (6) and (7) to update the matrix $\bar{\mathbf{H}}$(k).

Step IV. Smoothing the estimated angles

The Kalman gain and state covariance matrix are same as (20) and (21) respectively. The estimated state vector is given by

$$\hat{\mathbf{x}}(k \mid k) = \hat{\mathbf{x}}(k \mid k-1) + \mathbf{K}\Delta\bar{\mathbf{Y}}(k) \tag{38}$$

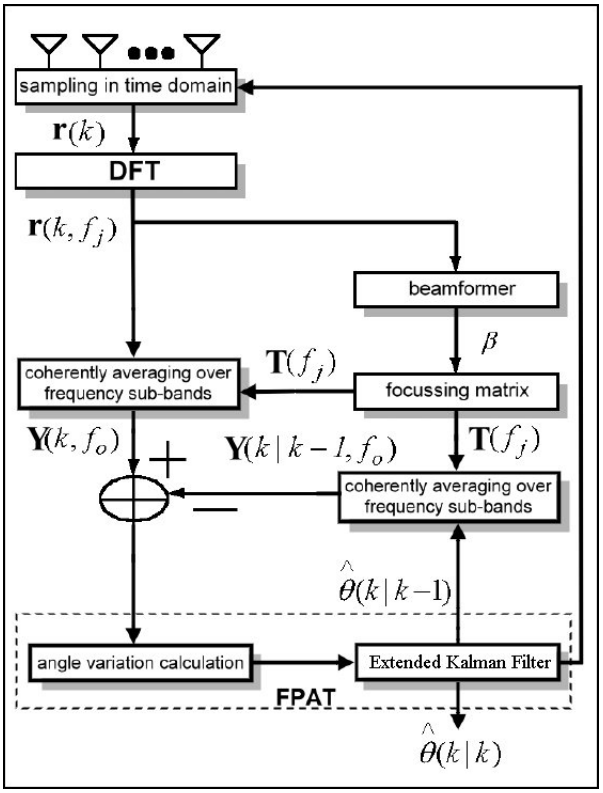

Fig. 2 The flow chart of the wideband FPAT tracking algorithm.

where $\Delta\bar{\mathbf{Y}}(k)=[\Delta\mathbf{Y}_R\ \Delta\mathbf{Y}_I]^T$, $\Delta\mathbf{Y}_R$ and $\Delta\mathbf{Y}_I$ are the real and imaginary parts of $\Delta\mathbf{Y}(k)$ from (37).

The flow chart of the wideband FPAT tracking algorithm is shown in Fig. 2. In this figure, a delay-and-sum beamformer is used to coarsely estimate the β angle in each group. These β angles are then used to form focusing matrices.

4 Computer Simulation Results

In this section, tracking performances of the three tracking algorithms are compared for narrowband sources in 2-D space. A uniform linear array of eight sensors M=8 with half wavelength as the interelement spacing is used. Three moving targets on the plane are tracked over an interval of 180s with T_s=1. During each T_s interval, L(=1, 10, 30, 50) snapshots of sensors data are generated. The Monte Carlo simulations of 100 runs were carried out for each algorithm with various SNRs. In all algorithms, the measurement noise covariance matrix $\mathbf{Q}$ and the process noise covariance matrix $\mathbf{R}$ are respectively set as $0.1\mathbf{I}$ and $0.2\mathbf{I}$, where $\mathbf{I}$ is the identity matrix. The weighting factors to constrain the absolute values of innovations in (17) are set to be $l_i=\frac{1}{20}\times$(i-th diagonal element of $\mathbf{B}^H\mathbf{B}$), which is the same as in Park's algorithm. The signal-to-noise ratio for the i-th target is defined as SNR=$10log(S_{ii}/\sigma^2)$, where S_{ii} is the (i,i) element of source covariance matrix $\mathbf{S}$ and σ^2 =0.1 is the noise variance.

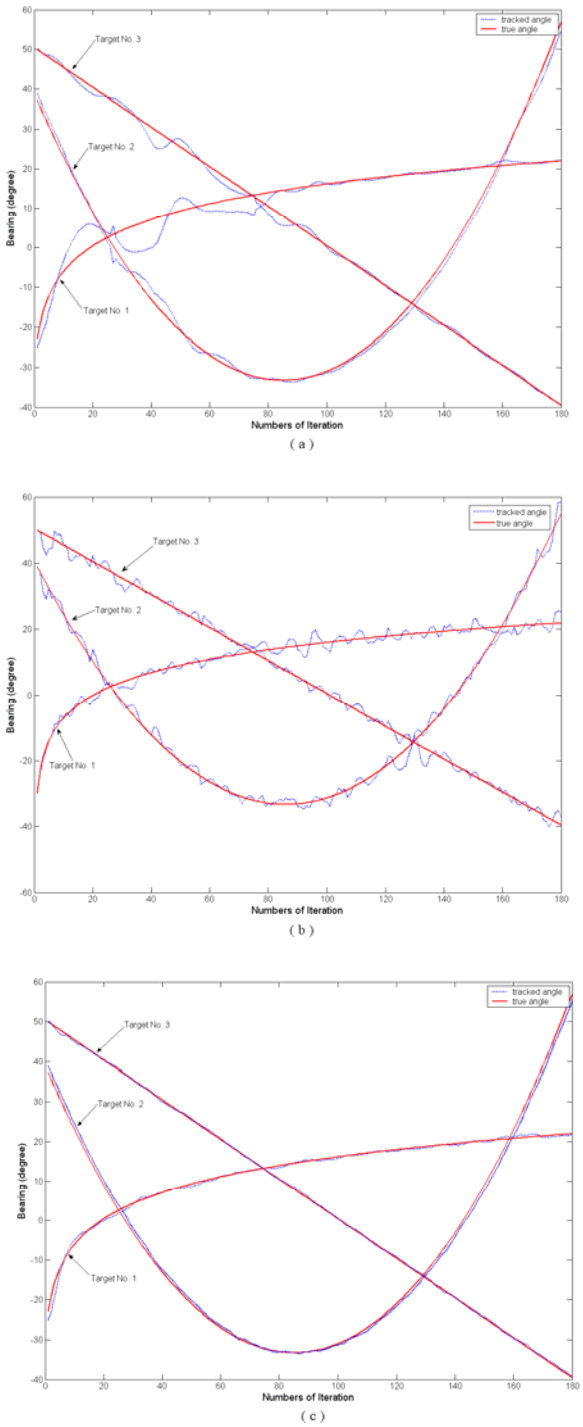

Fig. 3 Typical sample run for crossing tracks with three targets at SNR=10dB. (a)Kong's algorithm, (b)Park's agloritm, (c)FPAT algorithm.

Fig. 3 shows typical sample run for crossing tracks, all based on a single snapshot of data vector (L=1) at SNR=10dB of each target. The FPAT and Park's algorithms exhibit much better tracking capability than Kong's algorithm especially at the cross points in the trajectory.

Table 2 gives the tracking results for various SNRs at L=30 snapshots. The FPAT algorithm shows the highest tracking success rate (true angle ±5°) for each

SNRs. Table 3 presents the tracking results for various number of snapshots at SNR=10dB. Again, the proposed algorithm shows the highest tracking success rate for each number of snapshots.

Table 2. Tracking performance for various SNRs at snapshots=30.

SNR (dB)	Tracking success rate (%)		
	FPAT	Park's	Kong's
0	28	14	11
5	62	44	34
10	86	62	60

Table 3. Tracking performance for various number of snapshots at SNR=10dB.

Number of Snapshots	Tracking success rate (%)		
	FPAT	Park's	Kong's
1	70	45	43
10	83	69	55
50	88	81	66

Two moving targets are tracked over an interval of 20s with T_s=1 in 3-D space. During each T_s interval, L(=160) snapshots of sensors data are generated. Fig. 4 shows the tracking performances of the 3-D FPAT algorithm for the combinations of range, elevation, and azimuth at 3dB of SNR. In this figure, dot represents the true angle and line represents the tracked angle. The 3-D FPAT algorithm is very effective in tracking the targets in 3-D space, even at low SNR.

Two wideband coherent signals, with one being the delayed version of the other, are generated by passing a white Gaussion process through a 6^{th}-order Butterworth bandpass filter with the bandwidth of 40Hz and the center frequency of 100Hz. Both have the same power spectrum as shown in Fig. 5. The number of snapshots is 1024 and the sampling rate is 400 samples per second. Fig. 6 shows the tracking curves of the wide-band FPAT algorithm for the bearing of the two coherent wideband signals at 10dB of SNR. It is clear that by using the wideband FPAT method, the target angles are very accurately tracked.

5 Conclusion

We have presented the FPAT algorithm based on extended Kalman filter for tracking multiple targets. The proposed algorithm modified Park's algorithm by using the sensor array output vector rather than the sample covariance matrix and incorporating EKF instead of KF. These modifications allow the proposed algorithm to lower computational load, and

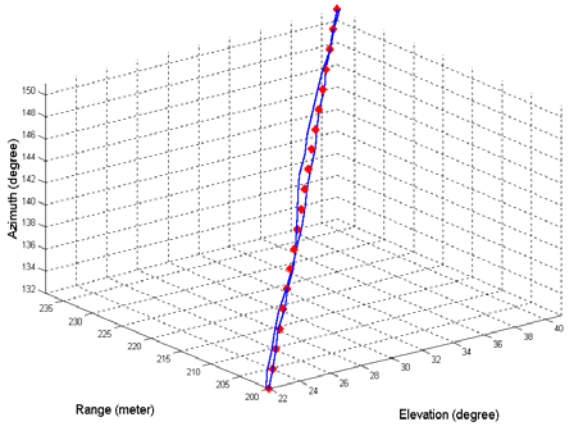

Fig. 4 The tracking curves of 3-D FPAT algorithm for the range, elevation, and azimuth of two targets at SNR=3dB.

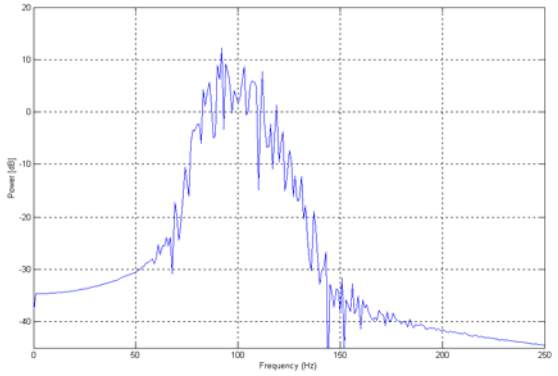

Fig. 5 The power spectrum of the wideband source with bandwidth of 40Hz and center frequency of 100Hz.

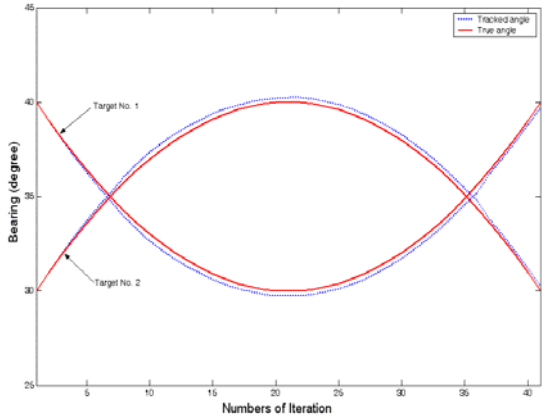

Fig. 6 The tracking curves of the wideband FPAT algorithm for the bearing angle of two wideband signals at SNR=10dB.

also improve the tracking success rate particularly at lower snapshots. The FPAT algorithm is then extnded to track the azimuth, elevation, and range of

multiple targets in 3-D space. Combined with the CSS method, the FPAT algorithm can be further extended to track wideband sources. Through computer simulations, the effectiveness of each proposed algorithm is demonstrated.

References:

[1] L. Ng, and Y. Bar-Shalom, Multisensor Multitarget Time Delay Vector Estimation, *IEEE Transactions on Acoustics, Speech, and Signal Processing*, ASSP-34, August 1986, pp. 669-677.

[2] J.-F. Yang, and M. Kaveh, Adaptive Eigensubspace Algorithms for Direction or Frequency Estimation and Tracking, *IEEE Transactions on Acoustics, Speech, and Signal Processing*, ASSP-36, February 1988, pp. 241-251.

[3] C. R. Sastry, E. W. Kamen, and M. Simaan, An Efficient Algorithm for Tracking the Angles of Arrival of Moving Targets, *IEEE Transactions on Acoustics, Speech and Signal Processing*, Vol. 39, No. 1, January 1991, pp. 242-246.

[4] C. K. Sword, M. Simaan, and E. W. Kamen, Multiple Target Angle Tracking Using Sensor Array Output, *IEEE Transactions on Aerospace and Electronic Systems*, Vol. 26, March 1990, pp. 367-372.

[5] P. Wang, and S. Wee, Sound Source Tracking Using Microphone Array, book chapter (Advances in Multimedia, Video and Signal Processing Systems), *WSEAS Press*, 2002, pp. 157-162.

[6] Nikos J. Farsaris, Angle of Arrival Target Tracking and Velocity Vector Determination Using SVD Method on Passive Coherent Multistatic Radar, *12th WSEAS Int. conf. on Communications*, July 2008, pp. 475-480.

[7] Nikos J. Farsaris, Thomas D. Xenos, Peter P. Stavroulakis, First Order Discrete Integrators for An Angle of Arrival Neural Network Target Detector on A Passive Multistatic Radar, *WSEAS Transactions on Communications*, Vol. 5, Issue 9, September 2006, pp. 1739-1743.

[8] Marta Marrón, Miguel Ángel Sotelo, Juan Carlos García, A Combined Stochastic-Deterministic Solution for Tracking Multiple Objects with An Stereo-Vision System, *WSEAS Transactions on Signal Processing*, Vol. 2, Issue 2, February 2006, pp. 253-260.

[9] C. R. Rao, C. R. Sastry, and B. Zhou, Tracking the Direction of Arrival of Multiple Moving Targets, *IEEE Transactions on Signal Processing*, Vol. 42, No. 5, May 1994, pp. 1133-1144.

[10] J. Sanchez-Araujo, and S. Marcos, An Efficient PASTd-Algorithm Implementation for Multiple Direction of Arrival Tracking, *IEEE Transactions on Signal Processing*, Vol. 47, No. 8, August 1999, pp. 2321-2324.

[11] S. B. Park, C. S. Ryu, and K. K. LEE, Multiple Target Angle Tracking Algorithm Using Predicted Angles, *IEEE Transactions on Aerospace and Electronic Systems*, Vol. 30, No. 2, April 1994, pp. 643-647.

[12] Chang-Soo Ryu, Sun-Hyoung Lee, and Kyun-Kyung Lee, Multiple Target Angle Tracking Algorithm Using Angular Innovations Extracted from Signal Subspace, *IEE Electronic Letters*, Vol. 35, No. 18, September 1999, pp. 1520-1522.

[13] Chang-Soo Ryu, Jang-Sik Lee, and Kyu-Kyung Lee, Multiple Target Angle-Tracking Algorithm with Efficient Equation for Angular Innovation, *IEE Electronic Letters*, Vol. 38, No. 10, May 2002, pp. 483-384.

[14] Yang Bin, Projection Approximaion Subspace Tracking, *IEEE Transactions on Signal Processing*, Vol. 43, No. 1, January 1995, pp. 95-107.

[15] Stephen C. Stubberud, Kathleen A. Kramer, Prognostic Target Tracking Accuracy of the Linearized Model Identified by the Neural Extended Kalman Filter, *WSEAS Transactions on System*, Vol. 3, Issue 9, November 2004, pp. 2782-2787.

[16] Dongkeon Kong, and Joohwan Chun, A Fast DOA Tracking Algorithm Based on the Extened Kalman Filter, *Proceeding of the IEEE NAECON Conf.*, October 2000, pp. 235-238.

[17] H. Wang, and M. Kaveh, Coherent Signal-Subspace Processing for the Detection and the Estimation of Angles of Arrival of Multiple Wide-band Sources, *IEEE Transactions on Acoustics, Speech and Signal Processing*, Vol. ASSP-33, August 1985, pp. 823-831.

[18] R. Schmidt, Multiple Emitter Location and Signal Parameter Estimation, *IEEE Transactions on Antennas, Propagation*, Vol. AP-34, No.3, March 1986, pp. 276-280.

[19] H. Hung, and M. Kaveh, Focussing Matrices for Coherent Signal-Subspace Processing, *IEEE Transactions on Acoustics, Speech and Signal Processing*, Vol. ASSP-36, August 1988, pp. 1272-1281.